Acta Cryst E CRYSTALLOGRAPHIC COMMUNICATIONS
ISSN 2056-9890

Structural characterization and antimycobacterial evaluation of a benzimidazole analogue of the antituberculosis clinical drug candidate TBA-7371

Adrian Richter,[a] Richard Goddard,[b] Roy Schönefeld,[a] Peter Imming[a] and Rüdiger W. Seidel[a]*

[a]Martin-Luther-Universität Halle-Wittenberg, Institut für Pharmazie, Wolfgang-Langenbeck-Str. 4, 06120 Halle (Saale), Germany, and [b]Max-Planck-Institut für Kohlenforschung, Kaiser-Wilhelm-Platz 1, 45470 Mülheim an der Ruhr, Germany. *Correspondence e-mail: ruediger.seidel@pharmazie.uni-halle.de

Received 21 October 2022
Accepted 1 November 2022

Edited by L. Van Meervelt, Katholieke Universiteit Leuven, Belgium

Keywords: benzimidazole; TBA-7371; scaffold morphing; DprE1 inhibitor; tuberculosis; crystal structure.

CCDC reference: 2216847

Supporting information: this article has supporting information at journals.iucr.org/e

The crystal structure and *in vitro* antimycobacterial properties of *N*-(2-fluoroethyl)-1-[(6-methoxy-5-methylpyrimidin-4-yl)methyl]-1*H*-benzo[*d*]imidazole-4-carboxamide ($C_{17}H_{18}FN_5O_2$, **1**), a previously reported benzimidazole analogue of the 1,4-azaindole-based antituberculosis drug candidate TBA-7371, are reported. The structure determination was achieved using Hirshfeld atom refinement. Compound **1** crystallizes in the triclinic system (space group $P\overline{1}$) with two molecules in the asymmetric unit ($Z' = 2$). The two crystallographically distinct molecules exhibit a similar conformation with the amide groups in a *Z* conformation, forming an intramolecular $N_{amide}—H\cdots N_{benzimidazole}$ hydrogen bond. The most significant supramolecular feature in the solid-state is a relatively short $C_{benzimidazole}—H\cdots N_{pyrimidine}$ hydrogen bond. Antimycobacterial testing confirmed *in vitro* activity against *Mycobacterium smegmatis*, but no growth inhibtion of *Mycobacterium abscessus* was found.

1. Chemical context

TBA-7371 (Fig. 1) is a 1,4-azaindole-based drug candidate for the treatment of tuberculosis, which has advanced to a Phase 2a clinical study (ClinicalTrials.gov identifier: NCT04176250). The compound is a non-covalent inhibitor of the mycobacterial enzyme decaprenylphosphoryl-β-D-ribose-2′-epimerase (DprE1), which is essential for cell-wall synthesis in *Mycobacterium tuberculosis*, the causative agent of tuberculosis (Shirude *et al.*, 2013, 2014; Chikhale *et al.*, 2018). As

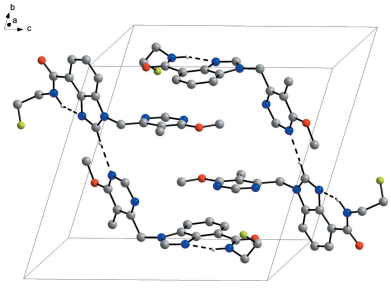

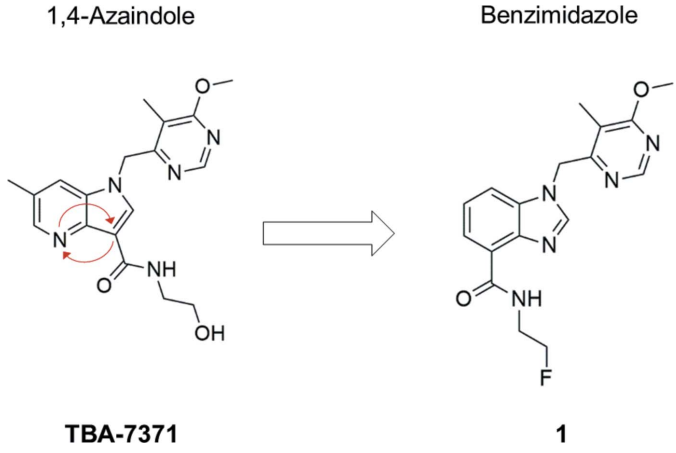

Figure 1
Scaffold morphing of 1,4-azaindole in TBA-7371 to benzimidazole in **1** (Manjunatha *et al.*, 2019).

shown in Fig. 1, scaffold morphing, a medicinal chemistry approach to the design of new ligands for the same target with a different core, led to the identification of *N*-(2-fluoroethyl)-1-[(6-methoxy-5-methylpyrimidin-4-yl)methyl]-1*H*-benzo[*d*]-imidazole-4-carboxamide (**1**) (Manjunatha *et al.*, 2019). In **1**, the 1,4-azaindole core has been replaced by a benzimidazole core, while the 6-methoxy-5-methylpyrimidine-4-yl group and the amide side chain were maintained. Compound **1** exhibits potent DprE1 inhibition and antimycobacterial activity (*vide infra*).

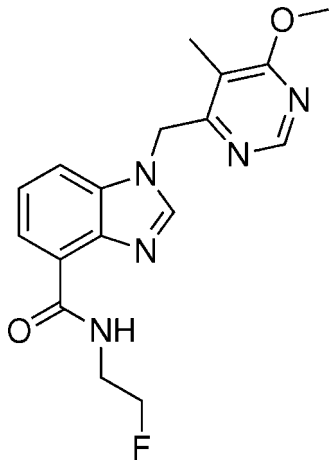

Late steps in the synthesis of **1**, following the previously published route (Manjunatha *et al.*, 2019), are sketched in Fig. 2. Benzimidazole derivative **A** was reacted with 4-(chloromethyl)-6-methoxy-5-methylpyrimidine to give **B**. It is worth mentioning that *N*-alkylation in part occurred at position 3 of the benzimidazole scaffold, affording side product **C**. Regioisomers **B** and **C** were separated by flash chromatography, resulting in an approximate 3.75:1 ratio.

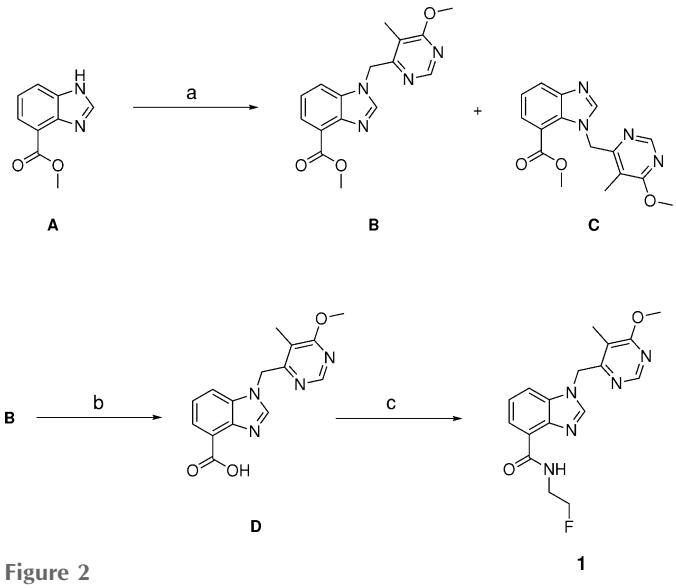

Figure 2
Synthesis of **1**, following the published procedure (Manjunatha *et al.*, 2019). Reagents and solvents: (*a*) 4-(chloromethyl)-6-methoxy-5-methylpyrimidine, Cs_2CO_3, NaI, DMF; (*b*) LiOH, MeOH; (*c*) HATU, 2-fluoroethanamine, NMP.

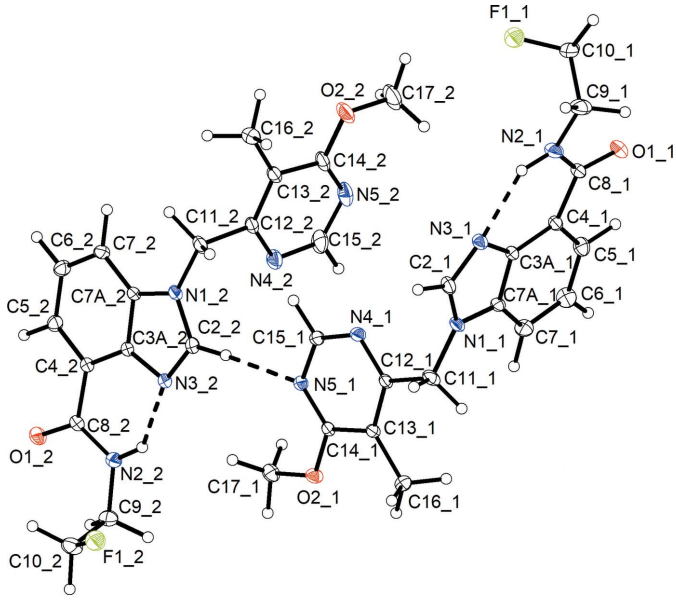

Figure 3
Asymmetric unit of **1**. Displacement ellipsoids are drawn at the 50% probability level. H atoms are represented by small spheres of arbitrary radius. Dashed lines represent hydrogen bonds. The number after the underscore indicates unique molecule 1 or 2.

Compound **C** was identified by ^{1}H and ^{13}C NMR spectroscopy and APCI mass spectrometry (see Supporting Information). Hydrolysis of **B** followed by amide coupling with 2-fluoroethanamine gave the target compound **1**. X-ray crystallography unambiguously confirmed the structure.

2. Structural commentary

Compound **1** crystallizes in the triclinic space group $P\overline{1}$ with two crystallographically distinct molecules (Fig. 3). In both molecules, the tilt of the 6-methoxy-5-methylpyrimidin-4-yl group of the plane out of the central benzimidazole moiety renders the conformers axially chiral. The C2—N1—C11—C12 torsion angle is 101.9 (1)° in molecule 1 and 79.0 (1)° in molecule 2. The enantiomeric conformers in the chosen asymmetric unit thus exhibit the same handedness, but the corresponding oppositely handed conformers are present in the centrosymmetric crystal structure. The most marked structural difference between the two unique molecules is the orientation of the 2-fluoroethyl group about the C9—C10 bond with N2—C9—C10—F1 = 68.1 (1)° for molecule 1 and −61.8 (1)° for molecule 2.

The plane of the amide group and the mean plane of the benzimidazole moiety are nearly co-planar in molecules 1 and 2. The angle between the two planes is 8.8 (1)° in molecule 1 and 7.7 (1)° in molecule 2. The amide group adopts a *Z* conformation in both molecules and forms an intramolecular N—H···H hydrogen bond to atom N3 of the benzimidazole system (Table 1), resulting in a six-membered hydrogen-bonded ring with an *S*(6) motif (Bernstein *et al.*, 1995). This is in line with Etter's second hydrogen-bond rule for organic compounds, which states that intramolecular six-membered

Table 1
Hydrogen-bond geometry (Å, °).

D—H···A	D—H	H···A	D···A	D—H···A
C2_1—H2_1···O1_2^{i}	1.054 (12)	2.353 (12)	3.2907 (14)	147.5 (9)
C7_1—H7_1···O1_2^{ii}	1.031 (12)	2.245 (13)	3.2211 (14)	157.4 (10)
N2_1—H2*a*_1···N3_1	1.002 (14)	2.035 (14)	2.8581 (14)	137.9 (10)
C2_2—H2_2···N5_1	1.060 (13)	2.240 (13)	3.2922 (15)	171.4 (9)
C7_2—H7_2···O1_1^{iii}	1.059 (12)	2.394 (12)	3.0915 (14)	122.3 (8)
C11_2—H11*b*_2···F1_1^{iv}	1.092 (12)	2.186 (12)	3.1839 (13)	150.7 (10)
C16_2—H16*c*_2···F1_2^{i}	1.047 (17)	2.403 (17)	3.2827 (15)	140.9 (12)
N2_2—H2*a*_2···N3_2	1.002 (14)	1.942 (14)	2.7823 (13)	139.6 (10)

Symmetry codes: (i) $-x+1, -y+1, -z$; (ii) $-x+2, -y+1, -z$; (iii) $-x+1, -y+1, -z+1$; (iv) $-x, -y+1, -z+1$.

hydrogen-bonded rings form in preference to intermolecular hydrogen bonds (Etter, 1990).

3. Supramolecular features

The most significant supramolecular feature of the title compound's solid-state structure is a short C—H···N contact between the amidine C2—H2 group of the benzimidazole moiety in molecule 2 and N5 of the pyrimidine ring in molecule 1 (Fig. 3), which provides structural evidence for a C—H···N weak hydrogen bond (Table 1). The amidine C2—H2 group in molecule 1 forms a short C—H···O contact to the amide carbonyl group of molecule 2. The geometric parameters including a D—H···A angle >140° (Wood *et al.*, 2009) are characteristic of a weak hydrogen bond (Thakuria *et al.*, 2017). F···F interactions are not encountered in the crystal structure, but parallel arrangements between the pyrimidine ring of molecule 1 and the benzimidazole moiety of a neighbouring molecule 2 (Fig. 4) and between the benzimidazole moieties of two molecules 1 about a center of symmetry are notable features (Fig. 5). The latter and the stacking of these units with the pyrimidine rings of molecule 2 in the b^*-axis direction no doubt contribute to the 040 reflection having by far the strongest intensity in the diffraction data set. A packing index of 71.9% (Kitaigorodskii, 1973), as calculated with *PLATON* (Spek, 2020), suggests that the solid-state structure appears to be mainly governed by close packing.

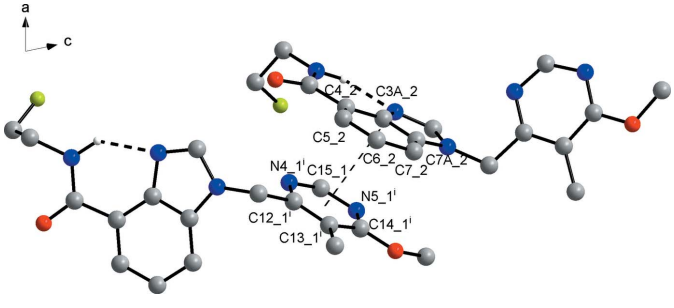

Figure 4
Section of the crystal structure of **1**, showing π–π stacking between the 6-methoxy-5-methylpyrimidin-4-yl moiety and the benzimidazole system in adjacent molecules. The distance between the centroids of the two six-membered rings (thin dashed line) is 3.6164 (11) Å. Thick dashed lines represent hydrogen bonds. Carbon-bound H atoms have been omitted for clarity. Symmetry code: (i) $-x+1, -y+1, -z$.

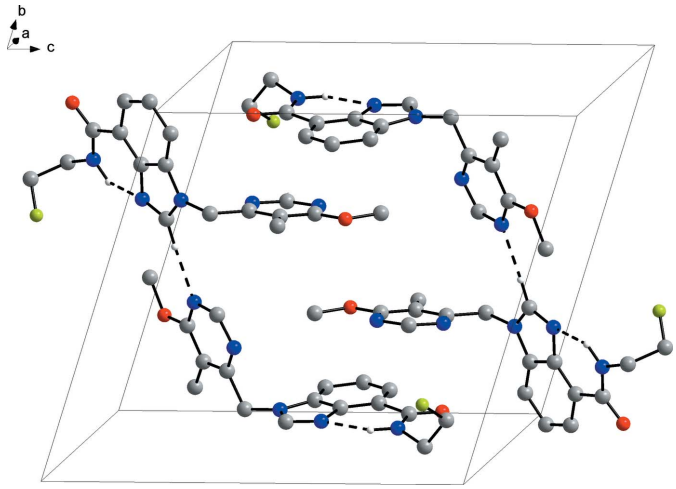

Figure 5
View of the triclinic unit cell of **1**, showing the stacking of benzimidazole and 6-methoxy-5-methylpyrimidin moieties in an *AABB* fashion in the b^*-axis direction. Dashed lines represent hydrogen bonds. H atoms have been omitted for clarity, except for amide and amidine H atoms.

4. Database survey

A search of the Cambridge Structural Database (CSD; Groom *et al.*, 2016) for acyclic 1-alkyl benzimidazole-4-carboxamides *via* WebCSD (accessed on 21 October 2022; CCDC, 2017) yielded the structure of 1-(2,6-difluorobenzyl)-2-(2,6-difluorophenyl)-1*H*-benzimidazole-4-carboxamide (Ziółkowska *et al.*, 2010; CSD refcode: PUMXAX). In PUMXAX, the amide group likewise forms an intramolecular N—H···N hydrogen bond to N3 of the benzimidazole system with an *S*(6) motif, and the 2,6-difluorobenzyl group and the benzimidazole moiety adopt an orientation to one another similar to that of the 6-methoxy-5-methylpyrimidin-4-yl group and the benzimidazole system in **1**.

A survey of crystal structures of the target enzyme DprE1 in the Protein Data Bank (PDB; Burley *et al.*, 2019), revealed that the conformation of the benzamide part of both molecules in **1** is similar to that of CT319, which is (*R*)-3-nitro-*N*-(1-phenylethyl)-5-(trifluoromethyl)benzamide, in the crystal structure of its non-covalent complex with *M. tuberculosis* DprE1 (PDB code: 4FDO; Batt *et al.*, 2012), as shown in Fig. 6.

5. Antimycobacterial evaluation

Manjunatha *et al.* (2019) reported an *in vitro* minimal inhibitory concentration (MIC) of 1.56–3.12 µM for **1** against *M. tuberculosis* H37Rv and MIC 0.78–1.56 µM against *Mycobacterium smegmatis*. Potent inhibition of the *M. tuberculosis* DprE1 and molecular docking suggested a mode of action similar to TBA-7371. We re-evaluated the *in vitro* activity of **1** against *M. smegmatis* mc^2 155, using broth microdilution assays (for the assay protocols, see supporting information and Richter *et al.*, 2018). We determined a MIC_{90} of 12.5 µM in Middlebrook 7H9 medium supplemented with 10% ADS (albumin-dextrose-saline) and 0.05% polysorbate 80, and

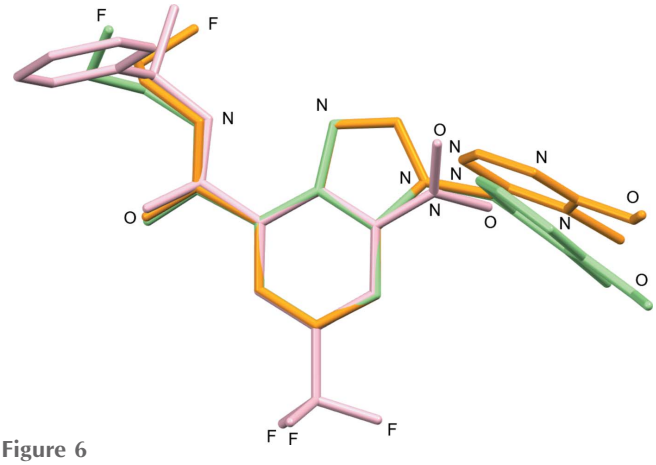

Figure 6
Structure overlay of the benzene rings of the two unique molecules of **1** (molecule 1: green; molecule 2: orange) and the benzene ring of CT319 in the crystal structure of its non-covalent complex with *M. tuberculosis* DprE1 (pink; PDB code: 4FDO; resolution: 2.4 Å), showing the similar conformations of the benzamide moieties.

6.25 µM in Mueller Hinton II Broth with 0.05% polysorbate 80.

The non-tuberculous *Mycobacterium abscessus* is an opportunistic pathogen, which can cause difficult-to-treat skin, soft tissue and pulmonary infections, in particular in patients with structural lung diseases such as cystic fibrosis (Boudehen & Kremer, 2021). Screening of antitubercular agents for activity against *M. abscessus* has been proposed (Ganapathy & Dick, 2022). Mechanism-based covalent DprE1 inhibitors with potent activity against *M. tuberculosis* and other mycobacteria like *M. smegmatis* form covalent adducts with the thiol group of Cys387 on the FAD substrate binding domain (Shetye *et al.*, 2020). These compounds are usually inactive against *M. abscessus*, since the *M. abscessus* DprE1 has an alanine residue in the corresponding amino-acid position, which prevents covalent linkage. Testing of non-covalent DprE1 inhibitors against *M. abscessus*, however, could be a promising approach to identifying potential lead structures. Therefore, we also tested **1** against *M. abscessus* ATCC19977 *in vitro*. In both Middlebrook 7H9 medium supplemented with 10% ADS and 0.05% polysorbate 80 and Mueller Hinton II Broth with 0.05% polysorbate 80, however, no growth inhibition could be detected (MIC_{90} > 100 µM). While this work was in progress, the same observation was reported for the parent 1,4-azaindole TBA-7371 (Sarathy *et al.*, 2022). It is worth noting, however, that Sarathy *et al.* (2022) found moderate *in vitro* activity against several *M. abscessus* strains and clinical isolates for the 3,4-dihydrocarbostyril-based non-covalent DprE1 inhibitor and Phase 2b/c clinical antituberculosis drug candidate OPC-167832.

6. Synthesis and crystallization

Compound **1** was synthesized as described by Manjunatha *et al.* (2019). Analytical data for **A**, **B**, **C** and **1** can be found in the supporting information. Crystals of **1** suitable for X-ray diffraction were grown from a solution in ethyl acetate/*n*-heptane (1:1) by slow evaporation of the solvents at room temperature.

Table 2
Experimental details.

Crystal data	
Chemical formula	$C_{17}H_{18}FN_5O_2$
M_r	343.36
Crystal system, space group	Triclinic, $P\overline{1}$
Temperature (K)	100
a, b, c (Å)	7.6940 (19), 15.013 (4), 15.281 (4)
α, β, γ (°)	71.040 (4), 77.874 (5), 87.780 (4)
V (Å^3)	1631.3 (7)
Z	4
Radiation type	Mo $K\alpha$
μ (mm^{-1})	0.10
Crystal size (mm)	0.10 × 0.05 × 0.02
Data collection	
Diffractometer	Bruker Kappa Mach3 *APEX*II
Absorption correction	Gaussian (*SADABS*; Krause *et al.*, 2015)
T_{min}, T_{max}	0.994, 0.999
No. of measured, independent and observed [$I \geq 2u(I)$] reflections	58016, 8147, 6141
R_{int}	0.048
(sin $\theta/\lambda)_{max}$ (Å^{-1})	0.671
Refinement	
$R[F^2 > 2\sigma(F^2)]$, $wR(F^2)$, S	0.031, 0.072, 1.07
No. of reflections	8147
No. of parameters	595
H-atom treatment	All H-atom parameters refined
$\Delta\rho_{max}$, $\Delta\rho_{min}$ (e Å^{-3})	0.34, −0.32

Computer programs: *APEX3* (Bruker, 2017), *SAINT* (Bruker, 2004), SHELXT (Sheldrick, 2015*a*), *OLEX2.refine* (Bourhis *et al.*, 2015), *DIAMOND* (Brandenburg, 2018), *Mercury* (Macrae *et al.*, 2020), *enCIFer* (Allen *et al.*, 2004) and *publCIF* (Westrip, 2010).

7. Refinement

Initially, the structure was refined to convergence using independent atom model refinement with *SHELXL2018/3* (Sheldrick, 2015*b*). The final structure refinement was carried out by Hirshfeld atom refinement with aspherical scattering factors using *NoSpherA2* (Kleemiss *et al.*, 2021; Midgley *et al.*, 2021) partitioning in *OLEX2* (Dolomanov *et al.*, 2009) based on electron density from iterative single-determinant SCF single-point DFT calculations using *ORCA* (Neese *et al.*, 2020) with a B3LYP functional (Becke, 1993; Lee *et al.*, 1988) and a def2-TZVPP basis set. Crystal data, data collection and structure refinement details are summarized in Table 2.

Acknowledgements

We are grateful to Professor Christian W. Lehmann for providing access to the X-ray diffraction facility at the Max-Planck-Institut für Kohlenforschung (Mülheim an der Ruhr, Germany) and Dr Nadine Taudte and Dr Jens-Ulrich Rahfeld for providing and maintaining the biosafety level 2 facility.

Funding information

This work was funded by the Deutsche Forschungsgemeinschaft (DFG, German Research Foundation) –

432291016, and supported by a financial grant from Mukoviszidose Institut gGmbH (Bonn, Germany), the research and development arm of the German Cystic Fibrosis Association Mukoviszidose e.V. We acknowledge the financial support within the funding programme Open Access Publishing by the DFG.

References

Allen, F. H., Johnson, O., Shields, G. P., Smith, B. R. & Towler, M. (2004). *J. Appl. Cryst.* **37**, 335–338.

Batt, S. M., Jabeen, T., Bhowruth, V., Quill, L., Lund, P. A., Eggeling, L., Alderwick, L. J., Fütterer, K. & Besra, G. S. (2012). *Proc. Natl Acad. Sci. USA*, **109**, 11354–11359.

Becke, A. D. (1993). *J. Chem. Phys.* **98**, 5648–5652.

Bernstein, J., Davis, R. E., Shimoni, L. & Chang, N.-L. (1995). *Angew. Chem. Int. Ed. Engl.* **34**, 1555–1573.

Boudehen, Y. M. & Kremer, L. (2021). *Trends Microbiol.* **29**, 951–952.

Bourhis, L. J., Dolomanov, O. V., Gildea, R. J., Howard, J. A. K. & Puschmann, H. (2015). *Acta Cryst.* A**71**, 59–75.

Brandenburg, K. (2018). *DIAMOND*. Crystal Impact GbR, Bonn, Germany.

Bruker (2004). *SAINT*. Bruker AXS Inc., Madison, Wisconsin, USA.

Bruker (2017). *APEX3*. Bruker AXS Inc., Madison, Wisconsin, USA.

Burley, S. K., Berman, H. M., Bhikadiya, C., Bi, C., Chen, L., DiCostanzo, L., Christie, C., Dalenberg, K., Duarte, J. M., Dutta, S., Feng, Z., Ghosh, S., Goodsell, D. S., Green, R. K., Guranović, V., Guzenko, D., Hudson, B. P., Kalro, T., Liang, Y., Lowe, R., Namkoong, H., Peisach, E., Periskova, I., Prlić, A., Randle, C., Rose, A., Rose, P., Sala, R., Sekharan, M., Shao, C., Tan, L., Tao, Y.-P., Valasatava, Y., Voigt, M., Westbrook, J., Woo, J., Yang, H., Young, J., Zhuravleva, M. & Zardecki, C. (2019). *Nucleic Acids Res.* **47**, D464–D474.

CCDC (2017). CSD web interface – intuitive, cross-platform, web-based access to CSD data. Cambridge Crystallographic Data Centre, Cambridge, England.

Chikhale, R. V., Barmade, M. A., Murumkar, P. R. & Yadav, M. R. (2018). *J. Med. Chem.* **61**, 8563–8593.

Dolomanov, O. V., Bourhis, L. J., Gildea, R. J., Howard, J. A. K. & Puschmann, H. (2009). *J. Appl. Cryst.* **42**, 339–341.

Etter, M. C. (1990). *Acc. Chem. Res.* **23**, 120–126.

Ganapathy, U. S. & Dick, T. (2022). *Molecules*, **27**, 6948.

Groom, C. R., Bruno, I. J., Lightfoot, M. P. & Ward, S. C. (2016). *Acta Cryst.* B**72**, 171–179.

Kitaigorodskii, A. I. (1973). *Molecular crystals and molecules.* London: Academic Press.

Kleemiss, F., Dolomanov, O. V., Bodensteiner, M., Peyerimhoff, N., Midgley, M., Bourhis, L. J., Genoni, A., Malaspina, L. A., Jayatilaka, D., Spencer, J. L., White, F., Grundkötter-Stock, B., Steinhauer, S., Lentz, D., Puschmann, H. & Grabowsky, S. (2021). *Chem. Sci.* **12**, 1675–1692.

Krause, L., Herbst-Irmer, R., Sheldrick, G. M. & Stalke, D. (2015). *J. Appl. Cryst.* **48**, 3–10.

Lee, C., Yang, W. & Parr, R. G. (1988). *Phys. Rev. B*, **37**, 785–789.

Macrae, C. F., Sovago, I., Cottrell, S. J., Galek, P. T. A., McCabe, P., Pidcock, E., Platings, M., Shields, G. P., Stevens, J. S., Towler, M. & Wood, P. A. (2020). *J. Appl. Cryst.* **53**, 226–235.

Manjunatha, M. R., Radha Shandil, R., Panda, M., Sadler, C., Ambady, A., Panduga, V., Kumar, N., Mahadevaswamy, J., Sreenivasaiah, M., Narayan, A., Guptha, S., Sharma, S., Sambandamurthy, V. K., Ramachandran, V., Mallya, M., Cooper, C., Mdluli, K., Butler, S., Tommasi, R., Iyer, P. S., Narayanan, S., Chatterji, M. & Shirude, P. S. (2019). *ACS Med. Chem. Lett.* **10**, 1480–1485.

Midgley, L., Bourhis, L. J., Dolomanov, O. V., Grabowsky, S., Kleemiss, F., Puschmann, H. & Peyerimhoff, N. (2021). *Acta Cryst.* A**77**, 519–533.

Neese, F., Wennmohs, F., Becker, U. & Riplinger, C. (2020). *J. Chem. Phys.* **152**, 224108.

Richter, A., Strauch, A., Chao, J., Ko, M. & Av-Gay, Y. (2018). *Antimicrob. Agents Chemother.* **62**, e00828–18.

Sarathy, J. P., Zimmerman, M. D., Gengenbacher, M., Dartois, V. & Thomas Dick, T. (2022). *bioRxiv* 2022.09.14.508059; doi: 10.1101/2022.09.14.508059.

Sheldrick, G. M. (2015*a*). *Acta Cryst.* A**71**, 3–8.

Sheldrick, G. M. (2015*b*). *Acta Cryst.* C**71**, 3–8.

Shetye, G. S., Franzblau, S. G. & Cho, S. (2020). *Transl. Res.* **220**, 68–97.

Shirude, P. S., Shandil, R., Sadler, C., Naik, M., Hosagrahara, V., Hameed, S., Shinde, V., Bathula, C., Humnabadkar, V., Kumar, N., Reddy, J., Panduga, V., Sharma, S., Ambady, A., Hegde, N., Whiteaker, J., McLaughlin, R. E., Gardner, H., Madhavapeddi, P., Ramachandran, V., Kaur, P., Narayan, A., Guptha, S., Awasthy, D., Narayan, C., Mahadevaswamy, J., Vishwas, K. G., Ahuja, V., Srivastava, A., Prabhakar, K. R., Bharath, S., Kale, R., Ramaiah, M., Choudhury, N. R., Sambandamurthy, V. K., Solapure, S., Iyer, P. S., Narayanan, S. & Chatterji, M. (2013). *J. Med. Chem.* **56**, 9701–9708.

Shirude, P. S., Shandil, R. K., Manjunatha, M. R., Sadler, C., Panda, M., Panduga, V., Reddy, J., Saralaya, R., Nanduri, R., Ambady, A., Ravishankar, S., Sambandamurthy, V. K., Humnabadkar, V., Jena, L. K., Suresh, R. S., Srivastava, A., Prabhakar, K. R., Whiteaker, J., McLaughlin, R. E., Sharma, S., Cooper, C. B., Mdluli, K., Butler, S., Iyer, P. S., Narayanan, S. & Chatterji, M. (2014). *J. Med. Chem.* **57**, 5728–5737.

Spek, A. L. (2020). *Acta Cryst.* E**76**, 1–11.

Thakuria, R., Sarma, B. & Nangia, A. (2017). *Hydrogen Bonding in Molecular Crystals.* In *Comprehensive Supramolecular Chemistry II*, vol. 7, edited by J. L. Atwood, pp. 25–48. Oxford: Elsevier.

Westrip, S. P. (2010). *J. Appl. Cryst.* **43**, 920–925.

Wood, P. A., Allen, F. H. & Pidcock, E. (2009). *CrystEngComm*, **11**, 1563–1571.

Ziółkowska, N. E., Michejda, C. J. & Bujacz, G. D. (2010). *J. Mol. Struct.* **966**, 53–58.

supporting information

Acta Cryst. (2022). E**78**, 1184-1188 [https://doi.org/10.1107/S2056989022010556]

Structural characterization and antimycobacterial evaluation of a benzimidazole analogue of the antituberculosis clinical drug candidate TBA-7371

Adrian Richter, Richard Goddard, Roy Schönefeld, Peter Imming and Rüdiger W. Seidel

Computing details

Data collection: *APEX3* (Bruker, 2017); cell refinement: *SAINT* (Bruker, 2004); data reduction: *SAINT* (Bruker, 2004); program(s) used to solve structure: SHELXT (Sheldrick, 2015a); program(s) used to refine structure: *olex2.refine* (Bourhis *et al.*, 2015); molecular graphics: *DIAMOND* (Brandenburg, 2018) and *Mercury* (Macrae *et al.*, 2020); software used to prepare material for publication: *enCIFer* (Allen *et al.*, 2004) and *publCIF* (Westrip, 2010).

N-(2-Fluoroethyl)-1-[(6-methoxy-5-methylpyrimidin-4-yl)methyl]-1,3-benzodiazole-4-carboxamide

Crystal data

$C_{17}H_{18}FN_5O_2$
M_r = 343.36
Triclinic, $P\overline{1}$
a = 7.6940 (19) Å
b = 15.013 (4) Å
c = 15.281 (4) Å
α = 71.040 (4)°
β = 77.874 (5)°
γ = 87.780 (4)°
V = 1631.3 (7) Å^3
Z = 4
$F(000)$ = 720
D_x = 1.398 Mg m^{-3}
Mo $K\alpha$ radiation, λ = 0.71073 Å
Cell parameters from 9963 reflections
θ = 2.7–28.2°
μ = 0.10 mm^{-1}
T = 100 K
Plate, colourless
0.10 × 0.05 × 0.02 mm

Data collection

Bruker AXS Kappa Mach3 APEX II diffractometer
Radiation source: Incoatec IμS
Incoatec Helios mirrors monochromator
Detector resolution: 66.67 pixels mm^{-1}
φ– and ω–scans
Absorption correction: gaussian (SADABS; Krause *et al.*, 2015)
T_{min} = 0.994, T_{max} = 0.999
58016 measured reflections
8147 independent reflections
6141 reflections with $I \geq 2u(I)$
R_{int} = 0.048
θ_{max} = 28.5°, θ_{min} = 1.4°
h = −10→10
k = −20→20
l = −20→19

Refinement

Refinement on F^2
Least-squares matrix: full
$R[F^2 > 2\sigma(F^2)]$ = 0.031
$wR(F^2)$ = 0.072
S = 1.07
8147 reflections
595 parameters
0 restraints
0 constraints
Primary atom site location: dual
Secondary atom site location: difference Fourier map

Hydrogen site location: inferred from neighbouring sites
All H-atom parameters refined

$w = 1/[\sigma^2(F_o^2) + (0.0302P)^2 + 0.1357P]$ where $P = (F_o^2 + 2F_c^2)/3$
$(\Delta/\sigma)_{max} = -0.001$
$\Delta\rho_{max} = 0.34$ e Å^{-3}
$\Delta\rho_{min} = -0.32$ e Å^{-3}

Special details

Experimental. Crystal mounted on a MiTeGen loop using Perfluoropolyether PFO-XR75.

Refinement. Refinement of F^2 against ALL reflections. The weighted R-factor wR and goodness of fit S are based on F^2, conventional R-factors R are based on F, with F set to zero for negative F^2. The threshold expression of $F^2 > 2\text{sigma}(F^2)$ is used only for calculating R-factors(gt) etc. and is not relevant to the choice of reflections for refinement. R-factors based on F^2 are statistically about twice as large as those based on F, and R- factors based on ALL data will be even larger.

Fractional atomic coordinates and isotropic or equivalent isotropic displacement parameters (Å^2)

	x	*y*	*z*	U_{iso}*/U_{eq}
C2_1	0.24678 (14)	0.11875 (7)	0.50249 (7)	0.0171 (2)
H2_1	0.1399 (16)	0.1169 (8)	0.4698 (8)	0.033 (3)*
C3A_1	0.40214 (12)	0.12795 (6)	0.60043 (7)	0.01224 (19)
C4_1	0.46666 (13)	0.12885 (6)	0.67969 (7)	0.0138 (2)
C5_1	0.64993 (14)	0.12841 (7)	0.67153 (8)	0.0188 (2)
H5_1	0.7017 (16)	0.1288 (9)	0.7320 (9)	0.037 (3)*
C6_1	0.76757 (14)	0.12644 (8)	0.58895 (8)	0.0223 (2)
H6_1	0.9064 (17)	0.1261 (8)	0.5876 (9)	0.040 (3)*
C7_1	0.70606 (13)	0.12396 (7)	0.51032 (8)	0.0187 (2)
H7_1	0.7946 (16)	0.1207 (8)	0.4507 (9)	0.038 (3)*
C7A_1	0.52267 (12)	0.12461 (6)	0.51864 (7)	0.0131 (2)
C8_1	0.35297 (14)	0.12221 (7)	0.77376 (7)	0.0175 (2)
C9_1	0.05871 (17)	0.09121 (8)	0.87354 (8)	0.0265 (3)
H9a_1	0.1274 (19)	0.0422 (11)	0.9242 (10)	0.057 (4)*
H9b_1	−0.0673 (19)	0.0628 (10)	0.8694 (10)	0.050 (4)*
C10_1	0.01296 (17)	0.17191 (8)	0.91114 (8)	0.0258 (3)
H10a_1	−0.0661 (19)	0.1461 (10)	0.9831 (11)	0.057 (4)*
H10b_1	0.1311 (18)	0.2145 (9)	0.9030 (9)	0.047 (4)*
C11_1	0.48068 (16)	0.10678 (7)	0.36547 (7)	0.0188 (2)
H11a_1	0.3719 (18)	0.0773 (9)	0.3485 (9)	0.044 (4)*
H11b_1	0.5883 (18)	0.0590 (9)	0.3682 (9)	0.048 (4)*
C12_1	0.54232 (13)	0.19816 (6)	0.28726 (7)	0.01278 (19)
C13_1	0.66938 (12)	0.19801 (6)	0.20828 (7)	0.01218 (19)
C14_1	0.70948 (12)	0.28746 (6)	0.13868 (6)	0.01223 (19)
C15_1	0.51185 (13)	0.35548 (7)	0.22720 (7)	0.0151 (2)
H15_1	0.4475 (15)	0.4202 (8)	0.2342 (8)	0.031 (3)*
C16_1	0.75853 (15)	0.11175 (7)	0.19506 (8)	0.0172 (2)
H16a_1	0.8798 (19)	0.1290 (10)	0.1421 (10)	0.054 (4)*
H16b_1	0.8024 (18)	0.0689 (10)	0.2556 (10)	0.052 (4)*
H16c_1	0.677 (2)	0.0719 (11)	0.1756 (10)	0.061 (4)*
C17_1	0.88043 (14)	0.38333 (7)	−0.00710 (7)	0.0181 (2)
H17a_1	0.9829 (17)	0.3724 (8)	−0.0611 (9)	0.040 (3)*

H17b_1	0.7668 (16)	0.4161 (8)	−0.0362 (8)	0.033 (3)*
H17c_1	0.9341 (16)	0.4290 (9)	0.0248 (9)	0.037 (3)*
N1_1	0.41820 (11)	0.11800 (5)	0.45741 (5)	0.01466 (17)
N2_1	0.17564 (12)	0.11793 (6)	0.78099 (6)	0.0202 (2)
H2a_1	0.1293 (17)	0.1211 (9)	0.7235 (10)	0.036 (4)*
N3_1	0.22925 (10)	0.12443 (6)	0.58814 (6)	0.01580 (18)
N4_1	0.46198 (11)	0.27632 (6)	0.29767 (6)	0.01515 (18)
N5_1	0.63354 (10)	0.36553 (5)	0.14786 (6)	0.01407 (17)
O1_1	0.41907 (11)	0.11614 (5)	0.84196 (5)	0.02732 (19)
O2_1	0.83091 (9)	0.29152 (5)	0.06084 (5)	0.01625 (15)
F1_1	−0.09275 (9)	0.23342 (5)	0.85713 (5)	0.0407 (2)
C2_2	0.63497 (13)	0.58977 (7)	0.02129 (7)	0.0161 (2)
H2_2	0.6202 (16)	0.5177 (9)	0.0635 (9)	0.038 (3)*
C3A_2	0.71862 (12)	0.72002 (6)	−0.08890 (7)	0.01256 (19)
C4_2	0.79584 (12)	0.79156 (7)	−0.17228 (7)	0.0130 (2)
C5_2	0.75312 (13)	0.88396 (7)	−0.17785 (7)	0.0161 (2)
H5_2	0.8156 (16)	0.9408 (9)	−0.2421 (9)	0.035 (3)*
C6_2	0.63746 (14)	0.90545 (7)	−0.10381 (7)	0.0188 (2)
H6_2	0.6057 (16)	0.9770 (9)	−0.1100 (8)	0.036 (3)*
C7_2	0.55929 (14)	0.83519 (7)	−0.02112 (7)	0.0171 (2)
H7_2	0.4735 (16)	0.8528 (8)	0.0344 (8)	0.034 (3)*
C7A_2	0.60227 (12)	0.74284 (7)	−0.01578 (7)	0.0140 (2)
C8_2	0.91827 (12)	0.77332 (7)	−0.25397 (7)	0.0138 (2)
C9_2	1.08197 (14)	0.65409 (8)	−0.31197 (8)	0.0188 (2)
H9a_2	1.1513 (16)	0.5933 (9)	−0.2806 (9)	0.039 (3)*
H9b_2	1.1762 (16)	0.7109 (9)	−0.3576 (9)	0.035 (3)*
C10_2	0.97648 (16)	0.62865 (9)	−0.37364 (8)	0.0269 (3)
H10a_2	0.8958 (17)	0.6864 (9)	−0.4029 (9)	0.044 (3)*
H10b_2	1.0606 (18)	0.6044 (9)	−0.4256 (10)	0.054 (4)*
C11_2	0.43832 (14)	0.64282 (8)	0.14634 (7)	0.0192 (2)
H11a_2	0.3521 (16)	0.5797 (9)	0.1648 (9)	0.039 (3)*
H11b_2	0.3542 (16)	0.7039 (9)	0.1409 (9)	0.038 (3)*
C12_2	0.54170 (13)	0.63169 (7)	0.22336 (7)	0.0154 (2)
C13_2	0.45344 (13)	0.63352 (7)	0.31175 (7)	0.0161 (2)
C14_2	0.56317 (15)	0.62089 (7)	0.37788 (7)	0.0201 (2)
C15_2	0.80399 (15)	0.60741 (8)	0.27110 (8)	0.0257 (3)
H15_2	0.9430 (17)	0.5958 (9)	0.2557 (9)	0.043 (3)*
C16_2	0.25762 (15)	0.64610 (8)	0.33854 (8)	0.0215 (2)
H16a_2	0.2278 (19)	0.6794 (10)	0.3907 (11)	0.061 (4)*
H16b_2	0.2055 (19)	0.6939 (11)	0.2826 (11)	0.063 (4)*
H16c_2	0.187 (2)	0.5814 (12)	0.3640 (11)	0.075 (5)*
C17_2	0.5973 (2)	0.61725 (10)	0.52889 (10)	0.0379 (3)
H17a_2	0.513 (2)	0.6183 (12)	0.5923 (13)	0.078 (5)*
H17b_2	0.6689 (18)	0.5546 (10)	0.5403 (10)	0.053 (4)*
H17c_2	0.691 (2)	0.6769 (12)	0.5007 (11)	0.063 (4)*
N1_2	0.54919 (11)	0.65749 (6)	0.05356 (6)	0.01600 (18)
N2_2	0.97000 (11)	0.68391 (6)	−0.23867 (6)	0.01570 (18)
H2a_2	0.9130 (17)	0.6344 (9)	−0.1783 (10)	0.034 (3)*

N3_2	0.73649 (10)	0.62313 (5)	−0.06356 (6)	0.01434 (17)
N4_2	0.71695 (11)	0.61835 (6)	0.20201 (6)	0.0216 (2)
N5_2	0.73631 (12)	0.60823 (6)	0.35843 (6)	0.0252 (2)
O1_2	0.96957 (9)	0.83717 (5)	−0.32943 (5)	0.01908 (16)
O2_2	0.48417 (11)	0.62231 (5)	0.46393 (5)	0.02792 (19)
F1_2	0.85963 (9)	0.55284 (5)	−0.31786 (5)	0.03320 (17)

Atomic displacement parameters (Å²)

	U^{11}	U^{22}	U^{33}	U^{12}	U^{13}	U^{23}
C2_1	0.0170 (5)	0.0220 (5)	0.0124 (5)	0.0007 (4)	−0.0054 (4)	−0.0044 (4)
C3A_1	0.0134 (5)	0.0129 (4)	0.0095 (5)	0.0004 (4)	−0.0016 (4)	−0.0029 (4)
C4_1	0.0163 (5)	0.0139 (5)	0.0113 (5)	0.0005 (4)	−0.0031 (4)	−0.0041 (4)
C5_1	0.0171 (5)	0.0217 (5)	0.0184 (6)	−0.0004 (4)	−0.0067 (4)	−0.0057 (4)
C6_1	0.0120 (5)	0.0290 (6)	0.0242 (6)	−0.0018 (4)	−0.0022 (4)	−0.0071 (5)
C7_1	0.0138 (5)	0.0211 (5)	0.0174 (5)	−0.0009 (4)	0.0025 (4)	−0.0045 (4)
C7A_1	0.0140 (5)	0.0130 (4)	0.0100 (5)	−0.0002 (4)	0.0005 (4)	−0.0024 (4)
C8_1	0.0251 (6)	0.0171 (5)	0.0112 (5)	0.0044 (4)	−0.0043 (4)	−0.0059 (4)
C9_1	0.0330 (7)	0.0225 (6)	0.0184 (6)	0.0017 (5)	0.0070 (5)	−0.0068 (5)
C10_1	0.0307 (7)	0.0269 (6)	0.0178 (6)	0.0104 (5)	0.0001 (5)	−0.0088 (5)
C11_1	0.0304 (6)	0.0133 (5)	0.0103 (5)	−0.0028 (4)	0.0001 (4)	−0.0030 (4)
C12_1	0.0182 (5)	0.0107 (4)	0.0090 (5)	−0.0004 (4)	−0.0029 (4)	−0.0026 (4)
C13_1	0.0141 (5)	0.0120 (5)	0.0104 (5)	−0.0004 (4)	−0.0017 (4)	−0.0039 (4)
C14_1	0.0141 (4)	0.0127 (5)	0.0097 (5)	−0.0003 (4)	−0.0026 (4)	−0.0032 (4)
C15_1	0.0187 (5)	0.0126 (5)	0.0122 (5)	0.0021 (4)	−0.0008 (4)	−0.0031 (4)
C16_1	0.0198 (5)	0.0142 (5)	0.0180 (6)	0.0025 (4)	−0.0038 (5)	−0.0061 (4)
C17_1	0.0174 (5)	0.0197 (5)	0.0137 (5)	−0.0031 (4)	0.0004 (4)	−0.0025 (4)
N1_1	0.0194 (4)	0.0146 (4)	0.0086 (4)	−0.0007 (3)	−0.0010 (3)	−0.0029 (3)
N2_1	0.0228 (5)	0.0221 (5)	0.0142 (5)	0.0016 (4)	0.0011 (4)	−0.0071 (4)
N3_1	0.0128 (4)	0.0217 (4)	0.0125 (4)	0.0016 (3)	−0.0019 (3)	−0.0055 (3)
N4_1	0.0195 (4)	0.0130 (4)	0.0116 (4)	0.0009 (3)	−0.0005 (3)	−0.0039 (3)
N5_1	0.0169 (4)	0.0126 (4)	0.0112 (4)	0.0009 (3)	−0.0016 (3)	−0.0027 (3)
O1_1	0.0369 (5)	0.0343 (4)	0.0155 (4)	0.0107 (4)	−0.0107 (3)	−0.0123 (3)
O2_1	0.0177 (3)	0.0157 (3)	0.0132 (3)	−0.0011 (3)	0.0013 (3)	−0.0044 (3)
F1_1	0.0328 (4)	0.0471 (5)	0.0366 (4)	0.0222 (3)	−0.0055 (3)	−0.0094 (3)
C2_2	0.0188 (5)	0.0155 (5)	0.0119 (5)	0.0025 (4)	−0.0030 (4)	−0.0017 (4)
C3A_2	0.0144 (5)	0.0129 (5)	0.0102 (5)	0.0018 (4)	−0.0036 (4)	−0.0031 (4)
C4_2	0.0147 (5)	0.0132 (5)	0.0113 (5)	0.0015 (4)	−0.0034 (4)	−0.0038 (4)
C5_2	0.0201 (5)	0.0125 (5)	0.0166 (5)	0.0007 (4)	−0.0058 (4)	−0.0048 (4)
C6_2	0.0226 (5)	0.0157 (5)	0.0211 (6)	0.0041 (4)	−0.0074 (4)	−0.0089 (4)
C7_2	0.0196 (5)	0.0204 (5)	0.0156 (5)	0.0057 (4)	−0.0063 (4)	−0.0105 (4)
C7A_2	0.0161 (5)	0.0168 (5)	0.0106 (5)	0.0041 (4)	−0.0046 (4)	−0.0059 (4)
C8_2	0.0150 (5)	0.0150 (5)	0.0111 (5)	−0.0010 (4)	−0.0027 (4)	−0.0035 (4)
C9_2	0.0164 (5)	0.0215 (6)	0.0190 (5)	0.0007 (4)	−0.0011 (4)	−0.0089 (5)
C10_2	0.0316 (6)	0.0330 (7)	0.0236 (6)	0.0063 (5)	−0.0092 (5)	−0.0176 (5)
C11_2	0.0171 (5)	0.0295 (6)	0.0107 (5)	0.0041 (5)	−0.0047 (4)	−0.0053 (4)
C12_2	0.0172 (5)	0.0181 (5)	0.0111 (5)	0.0019 (4)	−0.0051 (4)	−0.0035 (4)
C13_2	0.0224 (5)	0.0151 (5)	0.0116 (5)	−0.0004 (4)	−0.0055 (4)	−0.0041 (4)

C14_2	0.0316 (6)	0.0174 (5)	0.0135 (5)	−0.0012 (4)	−0.0111 (5)	−0.0040 (4)
C15_2	0.0198 (6)	0.0324 (6)	0.0247 (6)	0.0021 (5)	−0.0115 (5)	−0.0050 (5)
C16_2	0.0244 (6)	0.0236 (6)	0.0171 (6)	0.0016 (5)	−0.0027 (5)	−0.0085 (5)
C17_2	0.0664 (10)	0.0319 (7)	0.0231 (7)	0.0034 (7)	−0.0245 (7)	−0.0101 (6)
N1_2	0.0165 (4)	0.0205 (4)	0.0096 (4)	0.0041 (3)	−0.0026 (3)	−0.0036 (3)
N2_2	0.0163 (4)	0.0163 (4)	0.0142 (4)	0.0008 (3)	−0.0020 (3)	−0.0053 (4)
N3_2	0.0164 (4)	0.0147 (4)	0.0110 (4)	0.0031 (3)	−0.0026 (3)	−0.0033 (3)
N4_2	0.0181 (4)	0.0288 (5)	0.0173 (5)	0.0040 (4)	−0.0067 (4)	−0.0052 (4)
N5_2	0.0304 (5)	0.0259 (5)	0.0212 (5)	−0.0013 (4)	−0.0160 (4)	−0.0034 (4)
O1_2	0.0218 (4)	0.0182 (4)	0.0131 (4)	−0.0015 (3)	0.0001 (3)	−0.0015 (3)
O2_2	0.0457 (5)	0.0272 (4)	0.0147 (4)	0.0009 (4)	−0.0124 (4)	−0.0081 (3)
F1_2	0.0271 (4)	0.0315 (4)	0.0516 (5)	0.0002 (3)	−0.0106 (3)	−0.0262 (3)

Geometric parameters (Å, º)

C2_1—H2_1	1.054 (12)	C2_2—H2_2	1.060 (13)
C2_1—N1_1	1.3551 (13)	C2_2—N1_2	1.3599 (13)
C2_1—N3_1	1.3175 (13)	C2_2—N3_2	1.3133 (13)
C3A_1—C4_1	1.4063 (14)	C3A_2—C4_2	1.4043 (13)
C3A_1—C7A_1	1.4051 (13)	C3A_2—C7A_2	1.4042 (13)
C3A_1—N3_1	1.3871 (13)	C3A_2—N3_2	1.3877 (12)
C4_1—C5_1	1.3892 (14)	C4_2—C5_2	1.3926 (14)
C4_1—C8_1	1.4922 (14)	C4_2—C8_2	1.4929 (14)
C5_1—H5_1	1.082 (13)	C5_2—H5_2	1.101 (12)
C5_1—C6_1	1.3982 (15)	C5_2—C6_2	1.4029 (14)
C6_1—H6_1	1.064 (13)	C6_2—H6_2	1.070 (12)
C6_1—C7_1	1.3923 (16)	C6_2—C7_2	1.3910 (15)
C7_1—H7_1	1.031 (12)	C7_2—H7_2	1.059 (12)
C7_1—C7A_1	1.3898 (14)	C7_2—C7A_2	1.3932 (14)
C7A_1—N1_1	1.3834 (13)	C7A_2—N1_2	1.3812 (13)
C8_1—N2_1	1.3479 (14)	C8_2—N2_2	1.3448 (13)
C8_1—O1_1	1.2289 (12)	C8_2—O1_2	1.2346 (11)
C9_1—H9a_1	1.092 (15)	C9_2—H9a_2	1.064 (12)
C9_1—H9b_1	1.096 (14)	C9_2—H9b_2	1.090 (13)
C9_1—C10_1	1.5021 (16)	C9_2—C10_2	1.5073 (16)
C9_1—N2_1	1.4475 (14)	C9_2—N2_2	1.4450 (13)
C10_1—H10a_1	1.091 (15)	C10_2—H10a_2	1.078 (13)
C10_1—H10b_1	1.094 (14)	C10_2—H10b_2	1.066 (14)
C10_1—F1_1	1.3871 (13)	C10_2—F1_2	1.3989 (14)
C11_1—H11a_1	1.076 (14)	C11_2—H11a_2	1.102 (13)
C11_1—H11b_1	1.073 (13)	C11_2—H11b_2	1.092 (12)
C11_1—C12_1	1.5107 (14)	C11_2—C12_2	1.5169 (14)
C11_1—N1_1	1.4481 (13)	C11_2—N1_2	1.4456 (13)
C12_1—C13_1	1.3849 (13)	C12_2—C13_2	1.3869 (14)
C12_1—N4_1	1.3447 (12)	C12_2—N4_2	1.3422 (13)
C13_1—C14_1	1.4129 (13)	C13_2—C14_2	1.4111 (14)
C13_1—C16_1	1.4938 (14)	C13_2—C16_2	1.4974 (15)
C14_1—N5_1	1.3244 (12)	C14_2—N5_2	1.3228 (14)

C14_1—O2_1	1.3349 (11)	C14_2—O2_2	1.3344 (13)
C15_1—H15_1	1.100 (11)	C15_2—H15_2	1.066 (13)
C15_1—N4_1	1.3227 (13)	C15_2—N4_2	1.3289 (14)
C15_1—N5_1	1.3358 (13)	C15_2—N5_2	1.3305 (15)
C16_1—H16a_1	1.076 (14)	C16_2—H16a_2	1.055 (16)
C16_1—H16b_1	1.055 (14)	C16_2—H16b_2	1.063 (16)
C16_1—H16c_1	1.032 (16)	C16_2—H16c_2	1.047 (17)
C17_1—H17a_1	1.065 (13)	C17_2—H17a_2	1.051 (17)
C17_1—H17b_1	1.092 (12)	C17_2—H17b_2	1.055 (14)
C17_1—H17c_1	1.096 (13)	C17_2—H17c_2	1.083 (16)
C17_1—O2_1	1.4378 (12)	C17_2—O2_2	1.4341 (15)
N2_1—H2a_1	1.002 (14)	N2_2—H2a_2	1.002 (14)

N1_1—C2_1—H2_1	121.8 (6)	N1_2—C2_2—H2_2	121.1 (7)
N3_1—C2_1—H2_1	124.5 (6)	N3_2—C2_2—H2_2	125.3 (7)
N3_1—C2_1—N1_1	113.70 (9)	N3_2—C2_2—N1_2	113.60 (9)
C7A_1—C3A_1—C4_1	119.54 (8)	C7A_2—C3A_2—C4_2	120.12 (8)
N3_1—C3A_1—C4_1	130.61 (9)	N3_2—C3A_2—C4_2	130.02 (9)
N3_1—C3A_1—C7A_1	109.75 (8)	N3_2—C3A_2—C7A_2	109.86 (8)
C5_1—C4_1—C3A_1	117.17 (9)	C5_2—C4_2—C3A_2	117.23 (9)
C8_1—C4_1—C3A_1	124.80 (9)	C8_2—C4_2—C3A_2	123.55 (8)
C8_1—C4_1—C5_1	117.82 (9)	C8_2—C4_2—C5_2	119.22 (9)
H5_1—C5_1—C4_1	118.1 (6)	H5_2—C5_2—C4_2	117.9 (6)
C6_1—C5_1—C4_1	122.32 (10)	C6_2—C5_2—C4_2	121.84 (9)
C6_1—C5_1—H5_1	119.6 (6)	C6_2—C5_2—H5_2	120.2 (6)
H6_1—C6_1—C5_1	118.4 (7)	H6_2—C6_2—C5_2	120.5 (6)
C7_1—C6_1—C5_1	121.32 (10)	C7_2—C6_2—C5_2	121.47 (9)
C7_1—C6_1—H6_1	120.3 (7)	C7_2—C6_2—H6_2	118.0 (6)
H7_1—C7_1—C6_1	120.2 (7)	H7_2—C7_2—C6_2	120.4 (6)
C7A_1—C7_1—C6_1	116.21 (10)	C7A_2—C7_2—C6_2	116.54 (9)
C7A_1—C7_1—H7_1	123.5 (7)	C7A_2—C7_2—H7_2	123.1 (6)
C7_1—C7A_1—C3A_1	123.43 (9)	C7_2—C7A_2—C3A_2	122.79 (9)
N1_1—C7A_1—C3A_1	105.24 (8)	N1_2—C7A_2—C3A_2	105.16 (8)
N1_1—C7A_1—C7_1	131.26 (9)	N1_2—C7A_2—C7_2	132.05 (9)
N2_1—C8_1—C4_1	116.58 (9)	N2_2—C8_2—C4_2	115.46 (8)
O1_1—C8_1—C4_1	121.17 (9)	O1_2—C8_2—C4_2	121.45 (8)
O1_1—C8_1—N2_1	122.15 (10)	O1_2—C8_2—N2_2	123.08 (9)
H9b_1—C9_1—H9a_1	114.0 (11)	H9b_2—C9_2—H9a_2	110.2 (9)
C10_1—C9_1—H9a_1	105.0 (8)	C10_2—C9_2—H9a_2	107.5 (7)
C10_1—C9_1—H9b_1	106.5 (7)	C10_2—C9_2—H9b_2	107.5 (6)
N2_1—C9_1—H9a_1	108.6 (7)	N2_2—C9_2—H9a_2	109.5 (7)
N2_1—C9_1—H9b_1	109.1 (7)	N2_2—C9_2—H9b_2	109.8 (6)
N2_1—C9_1—C10_1	113.74 (10)	N2_2—C9_2—C10_2	112.27 (9)
H10a_1—C10_1—C9_1	109.9 (7)	H10a_2—C10_2—C9_2	110.4 (7)
H10b_1—C10_1—C9_1	111.7 (7)	H10b_2—C10_2—C9_2	111.2 (7)
H10b_1—C10_1—H10a_1	114.6 (10)	H10b_2—C10_2—H10a_2	113.6 (10)
F1_1—C10_1—C9_1	109.35 (10)	F1_2—C10_2—C9_2	108.97 (9)
F1_1—C10_1—H10a_1	106.5 (7)	F1_2—C10_2—H10a_2	106.7 (7)

F1_1—C10_1—H10b_1	104.4 (7)	F1_2—C10_2—H10b_2	105.6 (7)
H11b_1—C11_1—H11a_1	109.0 (10)	H11b_2—C11_2—H11a_2	108.4 (9)
C12_1—C11_1—H11a_1	108.2 (7)	C12_2—C11_2—H11a_2	109.4 (6)
C12_1—C11_1—H11b_1	108.6 (7)	C12_2—C11_2—H11b_2	109.5 (7)
N1_1—C11_1—H11a_1	107.6 (7)	N1_2—C11_2—H11a_2	108.5 (6)
N1_1—C11_1—H11b_1	109.8 (7)	N1_2—C11_2—H11b_2	106.9 (6)
N1_1—C11_1—C12_1	113.63 (8)	N1_2—C11_2—C12_2	113.96 (8)
C13_1—C12_1—C11_1	120.19 (8)	C13_2—C12_2—C11_2	119.79 (9)
N4_1—C12_1—C11_1	116.34 (8)	N4_2—C12_2—C11_2	117.08 (9)
N4_1—C12_1—C13_1	123.40 (8)	N4_2—C12_2—C13_2	123.11 (9)
C14_1—C13_1—C12_1	114.47 (8)	C14_2—C13_2—C12_2	114.56 (9)
C16_1—C13_1—C12_1	124.13 (9)	C16_2—C13_2—C12_2	124.46 (9)
C16_1—C13_1—C14_1	121.40 (9)	C16_2—C13_2—C14_2	120.97 (9)
N5_1—C14_1—C13_1	123.18 (9)	N5_2—C14_2—C13_2	123.50 (10)
O2_1—C14_1—C13_1	117.08 (8)	O2_2—C14_2—C13_2	116.73 (10)
O2_1—C14_1—N5_1	119.74 (8)	O2_2—C14_2—N5_2	119.77 (9)
N4_1—C15_1—H15_1	117.2 (6)	N4_2—C15_2—H15_2	117.0 (7)
N5_1—C15_1—H15_1	116.0 (6)	N5_2—C15_2—H15_2	115.9 (7)
N5_1—C15_1—N4_1	126.82 (9)	N5_2—C15_2—N4_2	127.12 (10)
H16a_1—C16_1—C13_1	111.8 (7)	H16a_2—C16_2—C13_2	111.5 (8)
H16b_1—C16_1—C13_1	113.0 (7)	H16b_2—C16_2—C13_2	113.1 (8)
H16b_1—C16_1—H16a_1	102.7 (10)	H16b_2—C16_2—H16a_2	101.5 (11)
H16c_1—C16_1—C13_1	111.6 (8)	H16c_2—C16_2—C13_2	111.4 (9)
H16c_1—C16_1—H16a_1	108.3 (11)	H16c_2—C16_2—H16a_2	108.5 (12)
H16c_1—C16_1—H16b_1	109.1 (11)	H16c_2—C16_2—H16b_2	110.3 (12)
H17b_1—C17_1—H17a_1	110.8 (9)	H17b_2—C17_2—H17a_2	110.4 (12)
H17c_1—C17_1—H17a_1	108.6 (9)	H17c_2—C17_2—H17a_2	111.0 (12)
H17c_1—C17_1—H17b_1	109.7 (9)	H17c_2—C17_2—H17b_2	108.9 (11)
O2_1—C17_1—H17a_1	105.9 (6)	O2_2—C17_2—H17a_2	106.2 (9)
O2_1—C17_1—H17b_1	110.8 (6)	O2_2—C17_2—H17b_2	110.5 (7)
O2_1—C17_1—H17c_1	111.0 (6)	O2_2—C17_2—H17c_2	109.9 (8)
C7A_1—N1_1—C2_1	106.63 (8)	C7A_2—N1_2—C2_2	106.66 (8)
C11_1—N1_1—C2_1	126.92 (9)	C11_2—N1_2—C2_2	126.10 (9)
C11_1—N1_1—C7A_1	126.35 (8)	C11_2—N1_2—C7A_2	126.98 (9)
C9_1—N2_1—C8_1	119.57 (10)	C9_2—N2_2—C8_2	122.13 (9)
H2a_1—N2_1—C8_1	118.7 (8)	H2a_2—N2_2—C8_2	118.6 (7)
H2a_1—N2_1—C9_1	120.7 (8)	H2a_2—N2_2—C9_2	118.4 (7)
C3A_1—N3_1—C2_1	104.67 (8)	C3A_2—N3_2—C2_2	104.70 (8)
C15_1—N4_1—C12_1	115.96 (8)	C15_2—N4_2—C12_2	115.91 (9)
C15_1—N5_1—C14_1	116.15 (8)	C15_2—N5_2—C14_2	115.79 (9)
C17_1—O2_1—C14_1	117.07 (8)	C17_2—O2_2—C14_2	116.88 (10)

C2_1—N1_1—C7A_1—C3A_1	0.69 (8)	C2_2—N1_2—C7A_2—C3A_2	1.07 (8)
C2_1—N1_1—C7A_1—C7_1	177.71 (8)	C2_2—N1_2—C7A_2—C7_2	−179.36 (8)
C2_1—N1_1—C11_1—C12_1	101.85 (10)	C2_2—N1_2—C11_2—C12_2	78.97 (10)
C2_1—N3_1—C3A_1—C4_1	−175.83 (7)	C2_2—N3_2—C3A_2—C4_2	−179.62 (7)
C2_1—N3_1—C3A_1—C7A_1	0.29 (8)	C2_2—N3_2—C3A_2—C7A_2	−0.08 (8)
C3A_1—C4_1—C5_1—C6_1	−0.47 (11)	C3A_2—C4_2—C5_2—C6_2	−0.20 (11)

C3A_1—C4_1—C8_1—N2_1	−2.07 (10)	C3A_2—C4_2—C8_2—N2_2	−8.31 (10)
C3A_1—C4_1—C8_1—O1_1	174.32 (10)	C3A_2—C4_2—C8_2—O1_2	172.85 (9)
C3A_1—C7A_1—C7_1—C6_1	0.27 (11)	C3A_2—C7A_2—C7_2—C6_2	0.26 (11)
C3A_1—C7A_1—N1_1—C11_1	−175.96 (7)	C3A_2—C7A_2—N1_2—C11_2	175.46 (7)
C4_1—C5_1—C6_1—C7_1	−0.58 (12)	C4_2—C5_2—C6_2—C7_2	−0.19 (12)
C4_1—C8_1—N2_1—C9_1	166.74 (9)	C4_2—C8_2—N2_2—C9_2	177.21 (8)
C5_1—C6_1—C7_1—C7A_1	0.67 (12)	C5_2—C6_2—C7_2—C7A_2	0.16 (11)
C6_1—C7_1—C7A_1—N1_1	−176.29 (8)	C6_2—C7_2—C7A_2—N1_2	−179.25 (8)
C7_1—C7A_1—N1_1—C11_1	1.06 (13)	C7_2—C7A_2—N1_2—C11_2	−4.97 (14)
C7A_1—N1_1—C11_1—C12_1	−82.17 (10)	C7A_2—N1_2—C11_2—C12_2	−94.36 (10)
C8_1—N2_1—C9_1—C10_1	84.98 (10)	C8_2—N2_2—C9_2—C10_2	−84.96 (10)
C11_1—C12_1—C13_1—C14_1	177.37 (9)	C11_2—C12_2—C13_2—C14_2	178.99 (10)
C11_1—C12_1—C13_1—C16_1	−2.24 (12)	C11_2—C12_2—C13_2—C16_2	−0.06 (12)
C11_1—C12_1—N4_1—C15_1	−177.50 (9)	C11_2—C12_2—N4_2—C15_2	−179.04 (10)
C12_1—C13_1—C14_1—N5_1	0.49 (10)	C12_2—C13_2—C14_2—N5_2	−0.01 (11)
C12_1—C13_1—C14_1—O2_1	−179.87 (8)	C12_2—C13_2—C14_2—O2_2	179.87 (9)
C12_1—N4_1—C15_1—N5_1	−0.46 (10)	C12_2—N4_2—C15_2—N5_2	0.03 (11)
C13_1—C14_1—N5_1—C15_1	−1.16 (11)	C13_2—C14_2—N5_2—C15_2	−0.37 (12)
C13_1—C14_1—O2_1—C17_1	−175.94 (9)	C13_2—C14_2—O2_2—C17_2	−175.04 (10)
C14_1—N5_1—C15_1—N4_1	1.18 (10)	C14_2—N5_2—C15_2—N4_2	0.38 (11)

Hydrogen-bond geometry (Å, º)

D—H···*A*	*D*—H	H···*A*	*D*···*A*	*D*—H···*A*
C2_1—H2_1···O1_2^{i}	1.054 (12)	2.353 (12)	3.2907 (14)	147.5 (9)
C7_1—H7_1···O1_2^{ii}	1.031 (12)	2.245 (13)	3.2211 (14)	157.4 (10)
N2_1—H2*a*_1···N3_1	1.002 (14)	2.035 (14)	2.8581 (14)	137.9 (10)
C2_2—H2_2···N5_1	1.060 (13)	2.240 (13)	3.2922 (15)	171.4 (9)
C7_2—H7_2···O1_1^{iii}	1.059 (12)	2.394 (12)	3.0915 (14)	122.3 (8)
C11_2—H11*b*_2···F1_1^{iv}	1.092 (12)	2.186 (12)	3.1839 (13)	150.7 (10)
C16_2—H16*c*_2···F1_2^{i}	1.047 (17)	2.403 (17)	3.2827 (15)	140.9 (12)
N2_2—H2*a*_2···N3_2	1.002 (14)	1.942 (14)	2.7823 (13)	139.6 (10)

Symmetry codes: (i) −*x*+1, −*y*+1, −*z*; (ii) −*x*+2, −*y*+1, −*z*; (iii) −*x*+1, −*y*+1, −*z*+1; (iv) −*x*, −*y*+1, −*z*+1.